Amplification of calcium signals at dendritic spines provides a method for CNS quantal analysis

Sabrina Wang, Oliver Prange, and Timothy H. Murphy

Abstract: It has been proposed that the small volume of a dendritic spine can amplify Ca^{2+} signals during synaptic transmission. Accordingly, we have performed calculations to determine whether the activation of *N*-methyl-D-aspartate (NMDA) type glutamate receptors during synaptic transmission results in significant elevation in intracellular Ca^{2+} levels, permitting optical detection of synaptic signals within a single spine. Simple calculations suggest that the opening of even a single NMDA receptor would result in the influx of ~ 310 000 Ca^{2+} ions into the small volume of a spine, producing changes in Ca^{2+} levels that are readily detectable using high affinity Ca^{2+} indicators such as fura-2 or fluo-3. Using fluorescent Ca^{2+} indicators, we have imaged local Ca^{2+} transients mediated by NMDA receptors in spines and dendritic shafts attributed to spontaneous miniature synaptic activity. Detailed analysis of these quantal events suggests that the current triggering these transients is attributed to the activation of <10 NMDA receptors. The frequency of these miniature synaptic Ca^{2+} transients is not randomly distributed across synapses, as some synapses can display a >10-fold higher frequency of transients than others. As expected for events mediated by NMDA receptors, miniature synaptic Ca^{2+} transients were suppressed by extracellular Mg^{2+} at negative membrane potentials; however, the Mg^{2+} block could be removed by depolarization.

Key words: miniature release, *N*-methyl-D-aspartate (NMDA), calcium, glutamate, spine.

Résumé : Des travaux ont suggéré que la petite taille d'une épine dendritique peut amplifier les signaux Ca^{2+} durant la transmission synaptique. Conséquemment, nous avons fait des calculs pour déterminer si l'activation des récepteurs du glutamate de type *N*-méthyl-D-aspartate (NMDA) durant la transmission synaptique provoque une augmentation significative des taux de Ca^{2+} intracellulaire, permettant la détection optique des signaux synaptiques à l'intérieur d'une seule épine. Des calculs simples suggèrent que l'ouverture d'un seul récepteur NMDA induirait un influx d'environ 310 000 ions Ca^{2+} dans une seule épine, provoquant des variations des taux de Ca^{2+} facilement détectables à l'aide d'indicateurs de Ca^{2+} de haute affinité comme le fura-2 ou le fluo-3. Nous avons utilisé des indicateurs de Ca^{2+} fluorescents pour examiner les fluctuations transitoires des courants Ca^{2+} locaux véhiculées par les récepteurs NMDA dans les épines et les axes dendritiques suite à une activité synaptique miniature spontanée. Une analyse détaillée de ces paramètres quantiques suggère que le courant déclenchant ces fluctuations transitoires est dû à l'activation de <10 récepteurs NMDA. Ces fluctuations ne sont pas distribuées aléatoirement à travers les synapses, étant donné que certaines synapses peuvent présenter une fréquence de fluctuations transitoires d'un facteur >10 supérieure à celle d'autres synapses. Comme prévu dans le cas des paramètres véhiculés par les récepteurs NMDA, les fluctuations transitoires des courants Ca^{2+} synaptiques ont été supprimées par les ions Mg^{2+} extracellulaires aux potentiels membranaires négatifs; toutefois, le blocage par les ions Mg^{2+} a pu être renversé par une dépolarisation.

Mots clés : mini-libération, *N*-méthyl-D-aspartate (NMDA), calcium, glutamate, épine.

[Traduit par la Rédaction]

Received August 24, 1998.

S. Wang and T.H. Murphy.[1] Kinsmen Laboratory of Neurological Research, Departments of Psychiatry and Physiology, Faculty of Medicine, The University of British Columbia, Vancouver, BC V6T 1Z3, Canada.
O. Prange. Kinsmen Laboratory of Neurological Research, Graduate Program in Neuroscience, Faculty of Medicine, The University of British Columbia, Vancouver, BC V6T 1Z3, Canada.

[1]Author for correspondence at the Kinsmen Laboratory of Neurological Research, Department of Psychiatry, Faculty of Medicine, The University of British Columbia, 2255 Wesbrook Mall, Vancouver, BC V6T 1Z3, Canada (e-mail: thmurphy@unixg.ubc.ca).

Introduction

Many models of synaptic physiology have focused on the dendritic spine as a structure that isolates or concentrates incoming synaptic signals (Lisman and Harris 1993; Harris and Kater 1994; Jaffe et al. 1994; Jaffe and Brown 1997; Edwards 1995; Segal 1995). The role of the dendritic spine in this function has remained somewhat controversial as some investigators propose a role for restriction of Ca^{2+} and not voltage. Computer modeling of Ca^{2+} dynamics (Zador et al. 1990; Koch et al. 1992; Koch and Zador 1993) has suggested that the dendritic spine would provide an ideal compartment to amplify Ca^{2+}-mediated signals. For example, Koch et al. (1992) proposed that at rest dendritic spines would contain only as few as 3 free calcium ions within

their small volume. This surprisingly small number is attributed to the fact that most Ca^{2+} ions are bound or buffered (1 free : 200 bound; Helmchen et al. 1996). Direct measurements of dendritic spine – shaft coupling by Svoboda et al. (1996) support the model of Koch and Zador (1993) and indicate a low spine neck resistance, suggesting little attenuation of voltage, but do not rule out a role in amplifying Ca^{2+} signals.

By using the fluorescent Ca^{2+} indicator fura-2 (Grynkiewicz et al. 1985), we have been able to detect optical signals attributed to the activation of a small number of *N*-methyl-D-aspartate (NMDA) receptors during miniature synaptic activity (Murphy et al. 1994, 1995). Yuste and Denk (1995), using acute hippocampal slices, also report similar Ca^{2+} transients mediated by miniature synaptic activity. We have focused on the study of spontaneous miniature synaptic activity since it permits a (optical) quantal analysis, by resolving the elemental form of synaptic transmission within a CNS neuron (Stevens 1993). Previous studies have shown that Ca^{2+} imaging can be used to resolve the activation of synaptic inputs during evoked activity (Regehr and Tank 1990; Muller and Connor 1991; Alford et al. 1993; Malinow et al. 1994; Yuste and Denk 1995; Schiller et al. 1998). In this manuscript we have extended our previous studies on the imaging of miniature synaptic activity by investigating in detail (*i*) the relationship between miniature synaptic currents and local changes in $[Ca^{2+}]_i$; (*ii*) the control of the frequency of miniature activity; and (*iii*) the voltage dependence of Ca^{2+} influx associated with miniature synaptic activity.

Methods

Embryonic cortical neurons and glial cells (from day-18 rat fetuses) were grown 3–4 weeks in vitro on polylysine-coated Aclar 33C (a nonfluorescent plastic substrate 0.127 mm thick) or glass cover slips before use in imaging experiments (as in Murphy and Baraban 1990). Aclar was obtained from Proplastics, Linden, N.J. Our animal protocol was approved by the Committee on Animal Care, The University of British Columbia (animal care certificate A95-0296) and followed the Canadian Council on Animal Care guidelines. Cultures were continuously perfused in a medium containing the following (in mM): NaCl, 137; KCl, 5.0; $CaCl_2$, 5.0; $MgSO_4$, 1; $Na_2HPO_4(7H_2O)$, 0.34; NaHepes buffer, 10; $NaHCO_3$, 1; tetrodotoxin, 0.0003–0.001; and glucose, 22 (pH 7.4 and ~315 mosmol). $MgSO_4$ levels were altered as indicated in the figure captions. Electrophysiological characteristics such as spike generation and input resistance of neurons prepared in this way have been previously described in Mackenzie and Murphy (1998). In some experiments (e.g., Fig. 1) 10–20 μM picrotoxin was added to suppress GABA receptors. A calculated liquid junction potential of 12 mV was not corrected for (Neher 1995*a*); therefore all membrane potentials and holding potentials are expected to be more negative than reported. In imaging experiments, we generally examined neurons that had holding currents of less than –200 pA at –80 mV. Additional criteria for selection of neurons included stable and low resting $[Ca^{2+}]_i$ levels and an absence of progressive morphological changes in dendrites, such as swelling. Because miniature synaptic currents were generally of low amplitude (see Fig. 1), series resistance compensation was not performed. For confocal imaging experiments the NMDA receptor blocker DL-2-amino-5-phosphonovaleric acid (DL-APV, 100 μM) was added during a baseline period (Fig. 2). In experiments requiring steady depolarization the L-type voltage-sensitive Ca^{2+} channel blocker PN200-110 (isradipine, 1 μM) was included in the perfusion medium (in some experiments another L-type blocker (R)PN202-791 (2 μM) was used instead of PN200-110). All experiments were conducted at room temperature (~23°C) in voltage clamp mode, with the exception of two experiments in which current clamp recording at about –70 mV membrane potential were performed. Imaging of neuronal Ca^{2+} transients was performed with wide field microscopy, using an intensified CCD camera, as previously described (Murphy et al. 1995; Mackenzie et al. 1996). Confocal imaging with a Bio-Rad MRC 600 system attached to a Zeiss upright (Axioskop) microscope was used for the experiments in Fig. 2 that required long sampling times. For the confocal imaging two objectives were used; either 0.9 N.A. Zeiss 63× water immersion or an Olympus 0.9 N.A. 60× water immersion. Confocal and video images were exported as byte arrays by removal of data headers and analyzed using custom routines written with the IDL (Research Systems Inc., Boulder, Colo.) programming language on a Pentium processor based computer. Whole-cell voltage and current clamp experiments (Hamill et al. 1981) were conducted using an Axon Instruments Axopatch 200B amplifier and 6–9 MΩ electrodes pulled from 1.5-mm glass pipettes. The patch pipettes were filled with a solution containing the following (in mM): fluo-3 K^+ salt, 0.5; K^+MeSO_4, 122; NaCl, 20; Mg-ATP, 5; GTP, 0.3; and Hepes, 10 (pH 7.2). In some cases K^+ was substituted with Cs^+ for better clamp control. In experiments using wide-field microscopy (Figs. 1 and 3), mag-fura-2, a low affinity Ca^{2+} indicator with high fluorescence at basal $[Ca^{2+}]_i$ at 380 nm excitation (Raju et al. 1989, 0.5–0.75 mM), was included in the pipette solution to resolve the fine processes under resting conditions. Fluo-3 and mag-fura-2 were purchased from Teflabs (Austin, Tex.). DL-APV was purchased from Precision Biochemicals Inc. (Vancouver, B.C.). Tetrodotoxin was purchased from Sigma Chemical Co. (St. Louis, Mo.). PN200-110 and (R)PN202-791 were gifts from Sandoz Research Institute (Hanover, N.J.).

For alignment of whole-cell current records with miniature synaptic calcium transients (MSCTs), we first determined the site and time of MSCT origin. The sites of MSCT origin were defined as previously described (Murphy et al. 1995) by monitoring the rising phase of the Ca^{2+} transient and selecting the dendritic region with the earliest rise. The initiation time of the Ca^{2+} transient was defined as the first point of four consecutive measurements (33-ms interval) that was 1 standard deviation above baseline noise. Alignment of currents would be limited by the 33-ms resolution of the imaging system. In some cases slow transient elevations in $[Ca^{2+}]_i$ were observed (>1 s rise time); these types of events were not considered MSCTs.

To identify dendritic regions showing MSCTs we used images of the change in fluo-3 fluorescence (difference images) between consecutive 1-s periods. For example, we first averaged fluorescence over 1-s periods (30 images) to obtain 10 averaged images (total sampling epoch is 10 s, 300 images). Images of change in fluorescence (difference images) were then produced by subtracting consecutive averaged images (image pairs) and determining their absolute value. The difference images were then averaged and a single image was created that reflected sites that exhibited greatest changes in fluorescence over the 10-s sampling epoch. These potential sites of MSCTs were further evaluated using plots from 2.0-μm^2 areas of interests (see Figs. 1 and 3).

In modeling Ca^{2+} influx into single spines we have assumed that 13.75% of the current carried by NMDA receptors is mediated by Ca^{2+} ions with 5 mM extracellular $CaCl_2$. We have based this assumption on the study of Garaschuk et al. (1996), who observed that 11% of the current (5.5% of the ions given the valence of 2) mediated by NMDA receptors was attributed to Ca^{2+} ions in 2.0 mM $CaCl_2$. Other assumptions were that the volume of a dendritic spine was 1 μm^3 (1×10^{-15} L). We have produced a simple

Fig. 1. A concentration of calcium signals in small dendritic compartments aides optical detection of quantal responses. (A) Schematic model of NMDA receptor mediated postsynaptic Ca^{2+} influx in response to presynaptic miniature transmitter release. Synaptic activation of a single NMDA receptor (given a 140-ms exponential decay of the current) will result on average in 310 000 Ca^{2+} ions entering the neuron; calculation based on charge transfer of the first 200 ms indicated by shaded area (see Methods). Cumulative charge transfer for the single-channel case is plotted above the simulated current for comparison with the actual current data shown in Fig. 1B. (B) Records of average change in fluo-3 fluorescence (dF) normalized to $F_{mag\text{-}fura\text{-}2}$ (F_{mag}: n = 25 MSCTs from both large and small processes) and corresponding averaged miniature synaptic current for 26 MSCTs recorded from the primary (1°) and secondary (2°; small diameter) dendrites of a cultured cortical neuron. (C) Cumulative miniature synaptic current plotted with average Ca^{2+} transient (data from fig. 1B). (D) Filtering of miniature synaptic current by dendritic processes. Miniature synaptic currents were localized to secondary (2°) or primary (1°) dendrites (n = 16 and 10, respectively) by using their temporal correlation with imaging data. Changes in fluo-3 fluorescence normalized to the fluorescence of a second fluorophore (mag-fura-2; F_{mag}) are plotted above the records of whole-cell current. Recordings were made in 5 mM $CaCl_2$, 0 $MgSO_4$ medium, at –80 mV holding potential in voltage clamp mode (R_s = 22 MΩ). The image shown in Fig. 1D is a raw mag-fura-2 image and depicts process architecture and volume of 1° and 2° dendrites, not changes in $[Ca^{2+}]_i$.

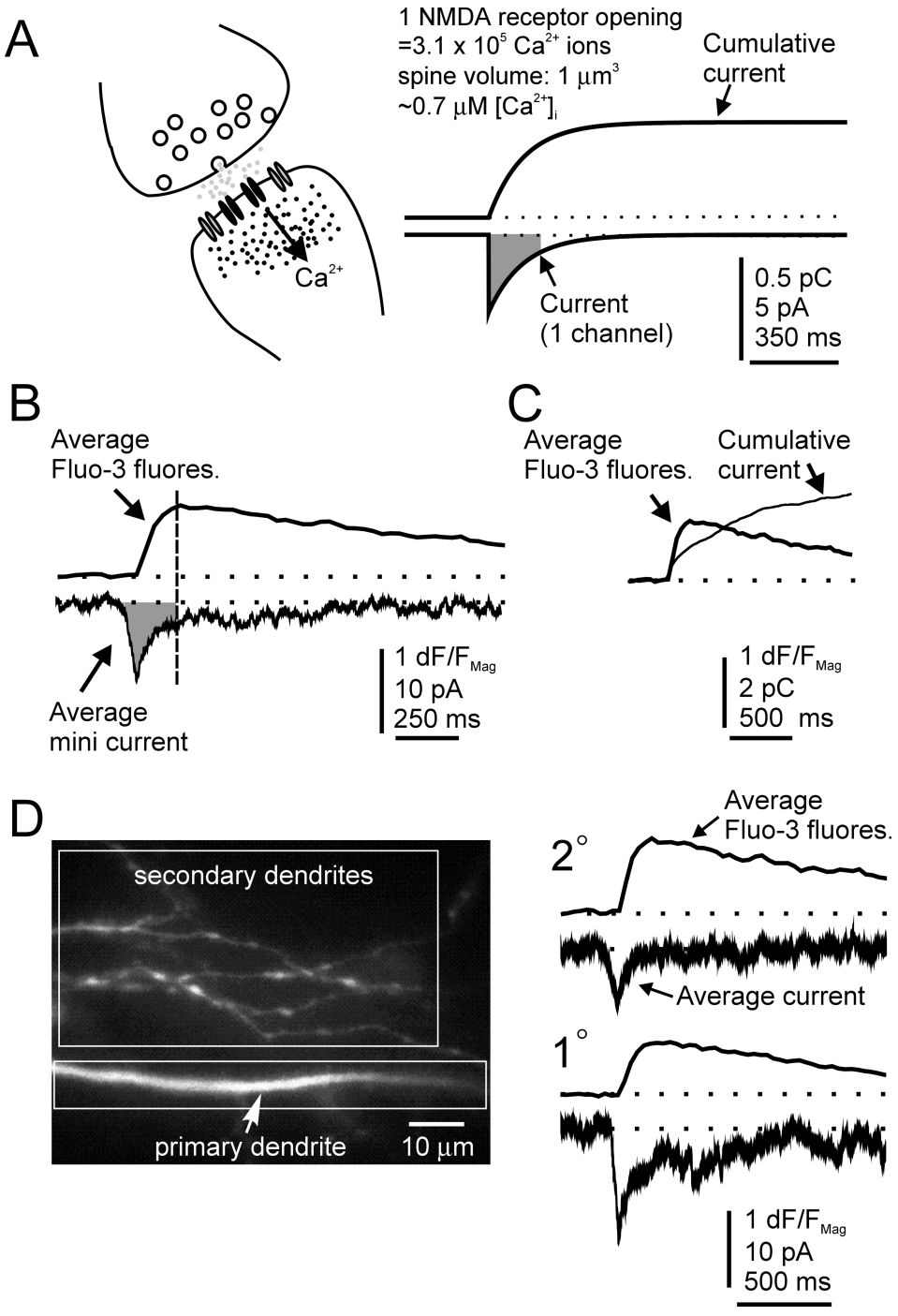

Fig. 2. Analysis of miniature synaptic Ca^{2+} transient frequency at single dendritic sites. (A) Example of MSCTs recorded using confocal microscopy. Left panel: Confocal image of dendrite region examined showing the location of the spines mentioned below. The image was produced by averaging fluo-3 fluorescence during baseline and MSCTs. Boxed regions correspond to magnified regions in middle panel (spines). Middle panel (spines): Three dendritic spines are highlighted, #1, #3, and # 4. Right panel: Plots of fluo-3 Ca^{2+}-induced fluorescence for seven dendritic sites. The data shown were obtained in medium nominally free of Mg^{2+} with 5 mM extracellular Ca^{2+} and at –80 mV holding potential under voltage clamp before and after washout of the NMDA antagonist DL-APV, using confocal microscopy with a 1.1-Hz sampling frequency. (B) Analysis of MSCT frequency using a Poisson distribution in the absence of extracellular $MgSO_4$. For each synapse the number of MSCTs observed per site was plotted. Expected values were generated using the Poisson equation ($p_{(k)} = (e^{-m} \cdot m^k)/k!$, where m is mean events/site and k is expected events/site). Comparison of the two distributions by the Kolmogorov–Smirnov distribution analysis test indicated that the Ca^{2+} transient frequencies were not described by a random Poisson distribution ($p < 3 \times 10^{-6}$). (C) Data reduction used to achieve a longer sampling period. An example of a high resolution record of fluo-3 fluorescence versus time (taken with a CCD camera at 30 Hz; trace 1) that was subjected to a simulated data reduction corresponding to the confocal sampling rate (1.1 Hz; trace 2). Despite this drastically reduced sampling rate, MSCTs were still detectable using the data reduction ($F_{red.}$, trace 2). To select responsive sites the first derivative of the fluorescence data ($F_{red.}$) was taken (dF/dt, trace 3). A response criterion was then applied; dF/dt responses must be greater than 2 SD of the baseline dF/dt. Data points that satisfy the criterion are shown in Fig. 2C (trace 4), labeled select.

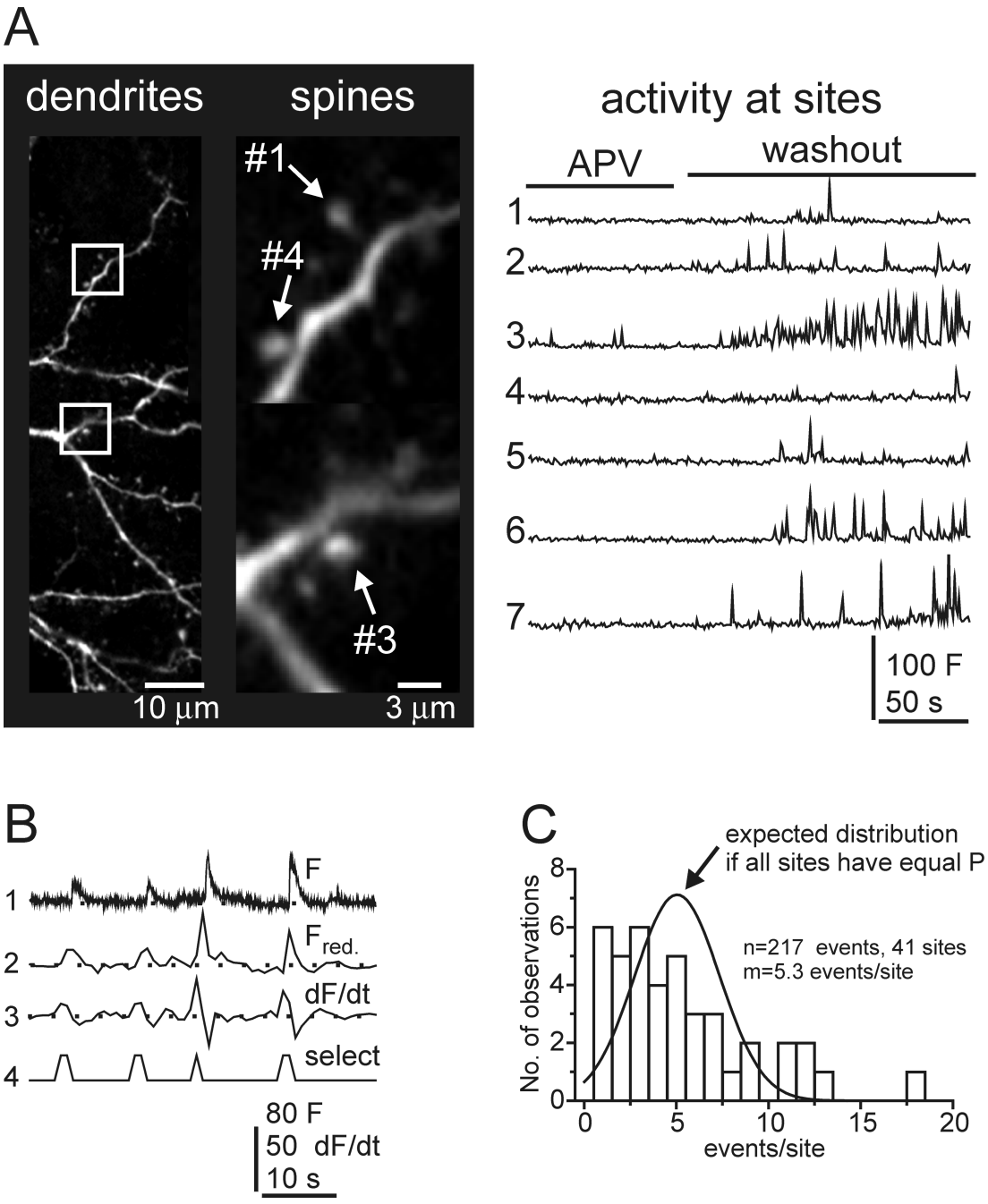

Fig. 3. Higher frequency and amplitude of miniature synaptic Ca^{2+} transients at depolarized potentials in the presence of extracellular Mg^{2+}. To examine the role of Mg^{2+} block in attenuating MSCTs in physiological extracellular Mg^{2+} (1 mM), MSCTs were compared at –35 and –80 mV holding potential under voltage clamp. A Ca^{2+} channel blocker was added to prevent a steady-state rise in $[Ca^{2+}]_i$ due to the depolarized potential (see Methods). At depolarized potentials, more frequent and larger Ca^{2+} transients were observed (all MSCT responses observed at each potential are plotted, as indicated), consistent with a role for NMDA receptors and removal of Mg^{2+} block (by depolarization). Occasionally, MSCTs were observed at negative membrane potentials (–80 mV). Examples of changes in fluorescence at –80 mV for four different dendritic sites (only responsive sites) are shown in the right panel. At one spine (records indicated by *) in particular a clear Ca^{2+} transient is observed at –80 mV (white box indicates enlarged region). However, at the other three sites, only small changes in fluorescence near background noise levels were observed (–80 mV). Three 10-s (300 image) epochs were obtained at –35 and –80 mV holding potentials. The image shown is of mag-fura-2 fluorescence (high fluorescence at resting Ca^{2+}) and depicts the process volume and structure. Dendritic locations of MSCTs were identified at each holding potential by analysis of serial difference images (1-s averages) as described in Methods.

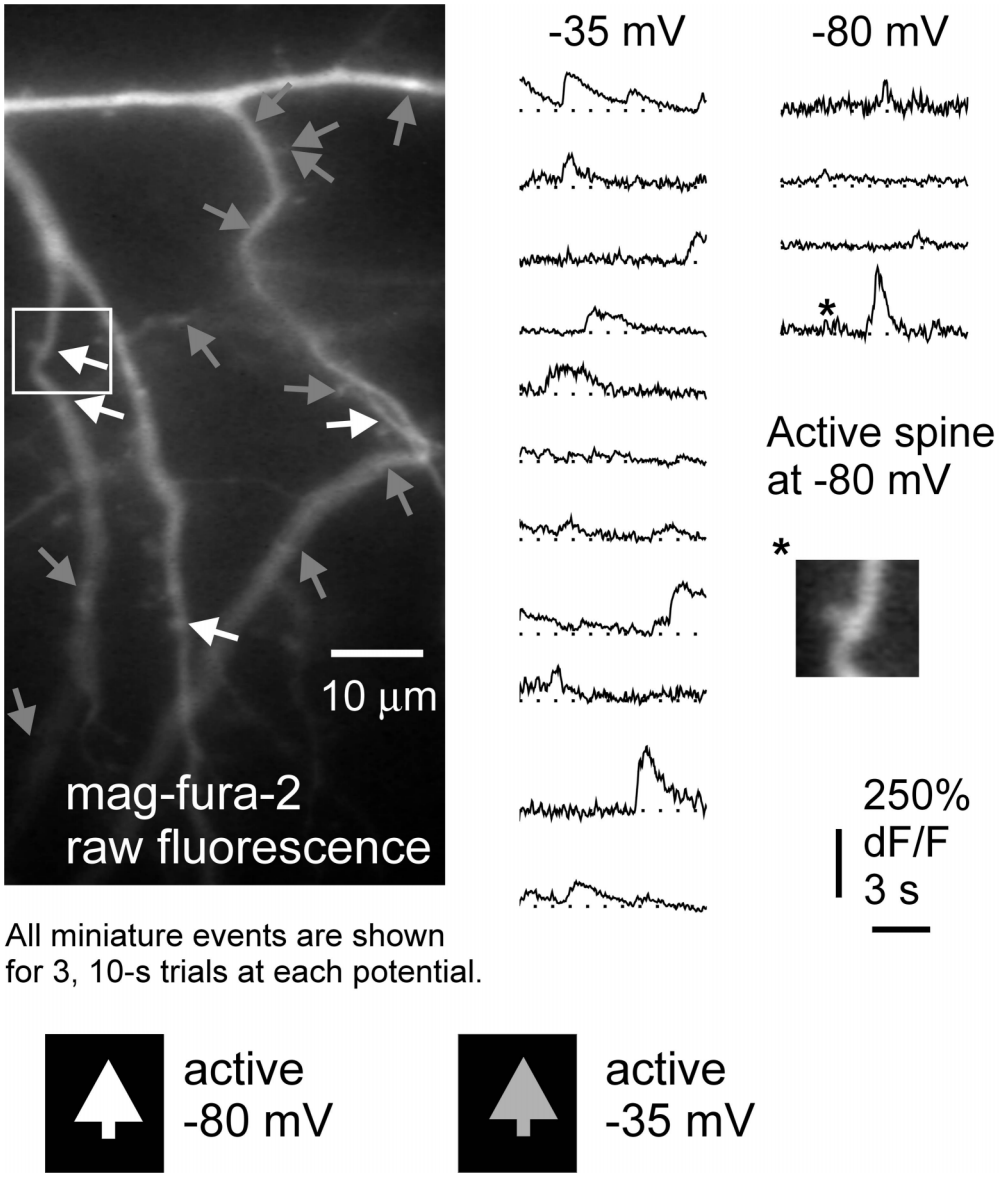

model for Ca^{2+} flux through NMDA receptors by assuming an instantaneous rise and an exponential decay of an NMDA receptor mediated miniature synaptic current (Fig. 1A). In our model we have used a decay time constant of 140 ms (determined from our data, Fig. 1B), resulting in a smooth curve that was scaled to an amplitude predicted for opening of a single NMDA receptor channel (McBain and Mayer 1994). This smooth curve was used to approximate the average Ca^{2+} flux through a single receptor. Although this smooth curve with an instantaneous rise would not mimic the slow activation (~10 ms rise time) and the stochastic behavior of NMDA receptors, it would approximate the shape of the NMDA receptor mediated excitatory postsynaptic current (EPSC) (Lester et al. 1990). Errors in Ca^{2+} influx attributed to using an instantaneous rise of NMDA receptor current would be small given the prolonged time course of the NMDA receptor EPSC. To estimate the $[Ca^{2+}]_i$ levels associated with the average kinetics and ion flux of a single NMDA receptor opening, we calculated the average current over the first 200 ms after receptor activation (1.9 pA).

This value was then converted to charge (1.9 pC/s × 0.2 s = 0.38 pC), and the charge was converted to ions (using 6.02×10^{18} ions/C). Assuming that 13.75% of the ions are Ca^{2+} (as above) we estimate that 310 000 Ca^{2+} ions enter the spine (on average) during the opening of a single channel over 200 ms. Assuming that Ca^{2+} buffering is on the order of 1 ion free to 200 bound in dendrites of mammalian forebrain neurons (Helmchen et al. 1996), we estimate 2.6 μM free $[Ca^{2+}]_i$ (for a spine volume of 1×10^{-15} L). In addition to buffers, Ca^{2+} extrusion mechanisms need to be considered. Based on the model of Schneggenburger et al. (1993, equation 8) and assuming a linear (first order) Ca^{2+} extrusion mechanism with a time constant of 80 ms (Helmchen et al. 1996), we estimate $[Ca^{2+}]_i$ of ~0.7 μM in a spine on average 200 ms after the activation of a single NMDA receptor. We have estimated $[Ca^{2+}]_i$ after the activation of a single NMDA receptor to represent the limit of optical detection. It is likely that this $[Ca^{2+}]_i$ is an overestimate since we have assumed no diffusion of Ca^{2+} out of the spine neck. We also acknowledge that Ca^{2+} buffering or extrusion mechanisms in spines may be greater than those measured in dendrites (Helmchen et al. 1996), also resulting in an overestimate of free $[Ca^{2+}]_i$ levels.

Results

Measurements of miniature synaptic currents indicate that a small number of NMDA receptors (<8) are activated during quantal transmission (Bekkers and Stevens 1989; Robinson et al. 1991; Silver et al. 1992). With regard to Ca^{2+}, we estimate that even the opening of a single NMDA receptor in the absence of Mg^{2+} block results in the influx of ~ 310 000 Ca^{2+} ions into the synapse (Fig. 1A). Given a dendritic spine volume of 1 μm^3 or less, we estimate $[Ca^{2+}]_i$ to be elevated to ~0.7 μM levels (Fig. 1A and Methods). These rather large changes in $[Ca^{2+}]_i$ would be detectable using high affinity fluorescent Ca^{2+} indicators (Grynkiewicz et al. 1985; Minta et al. 1989). Consistent with this proposal, we have previously filled neurons with fura-2, and have shown detection of the Ca^{2+} component of spontaneous miniature synaptic activity, termed miniature synaptic calcium transients (MSCTs; Murphy et al. 1994, 1995). In these experiments it is important to use a high concentration of Ca^{2+} indicator (0.3–0.5 mM) to detect the small dendritic spines over background fluorescence. A high indicator concentration also ensures efficient capture of incoming Ca^{2+} ions, resulting in a fluorescent signal that is proportional to Ca^{2+} influx (Neher 1995*b*). We now report a detailed analysis of the average current that triggers these MSCTs.

In Fig. 1B, a plot of the average miniature synaptic current and associated changes in fluo-3 fluorescence from 26 miniature synaptic events recorded from single synaptic sites within a single neuron is shown. Examination of the rise time of the Ca^{2+} transient versus that of the current indicated a lag in reaching peak Ca^{2+} levels (when compared with the peak current). To further examine this lag we plotted the cumulative current versus the change in Ca^{2+}-induced fluorescence, and observed that Ca^{2+} influx (synaptic current) continues even after peak fluorescence is reached (Fig. 1C). This result indicated that the slow peak of the MSCT (~150 ms) could be attributed to current still coming into the synapse during the decay phase of the EPSC. Selection of synapses that were on large-diameter dendritic processes (>3 μm) and within 50–100 μm of the neuronal soma (to reduce potential effects of dendritic filtering) suggested that we were not greatly underestimating the amplitude of the currents that were coinciding with MSCTs (Fig. 1D). Our analysis indicated that on average very small currents trigger MSCTs. For example, the average amplitude of the miniature current that was temporally correlated with the $[Ca^{2+}]_i$ transient was ~10 pA for synapses that were close to the cell body (Fig. 1D). If one assumes no dendritic filtering of responses, this would be accounted for by opening as few as three NMDA receptor channels (see Fig. 1A for average current through single channel). The sensitivity of MSCTs to NMDA receptor antagonists (see Fig. 2 and Murphy et al. 1994) suggests that MSCTs are predominantly mediated by NMDA receptors. When monitoring responses at the cell soma, one must consider some modest filtering of synaptic current due to pipette series resistance (~22 MΩ for the example in Fig. 1) and dendritic cable properties (Spruston et al. 1994). Recent data by Forti et al. (1997) suggest filtering of synaptic current amplitude measured by somatic whole cell recording by up to 70%. Therefore, if we estimate filtering of up to 70%, the average current we observe would be attributed to the activation of as few as 10 NMDA receptors. The effects of dendritic filtering were apparent when currents that correlated with local changes in $[Ca^{2+}]_i$ were compared in primary and secondary dendrites (Fig. 1D). In the case of activity at secondary dendrites, changes in $[Ca^{2+}]_i$ were comparable with those at the primary dendrite (when expressed as a dF/F_{mag}). However, the average amplitude of the miniature current (measured by the integral) was larger on the primary dendrite, suggesting filtering of currents on secondary dendritic processes (Fig. 1D).

Previous results from our laboratory have suggested a nonrandom distribution of MSCTs across synaptic sites (Murphy et al. 1994, 1995). However, these experiments were limited to rather short sampling times as a result of data storage restrictions and potential for cell damage due to excessive light exposure. To overcome this limitation, data from multiple cells were pooled (Murphy et al. 1994). We have now used confocal microscopy and slower sampling rates to compare the frequency of MSCTs at different synapses within a single neuron over relatively long periods (Fig. 2A). Using confocal microscopy we show that even with a slow sampling rate (1.1 Hz), we are able to reliably detect MSCTs (Fig. 2B). Proof of this was made by performing a simulated data reduction of MSCTs recorded with high temporal resolution (30 Hz; CCD camera data) to the 1.1-Hz temporal resolution associated with confocal imaging. This simulation shows that a lower sampling rate is still able to detect these events (see example in Fig. 2B).

In the example shown in Fig. 2A, seven dendritic sites were examined for MSCTs, using confocal microscopy. For these sites plots of raw fluorescence (pixel value) versus time are shown. Examination of confocal images of fluo-3 fluorescence indicated that the transients show characteristics that were consistent with MSCTs (data not shown). In the presence of the NMDA receptor antagonist DL-APV (100 μM) most sites, with the exception of site 3, show little or no spontaneous changes in $[Ca^{2+}]_i$. At some dendritic sites a large number of spontaneous $[Ca^{2+}]_i$ transients (MSCTs) were observed after washout of DL-APV (Fig. 2A). The MSCT frequency after DL-APV washout varied considerably (in some cases >10-fold) between spines (e.g., compare spines 1 and 3). To further analyze these events, we

constructed a distribution of MSCT frequencies for this neuron. Only dendritic sites that showed events are included in this analysis (no inactive sites were included). The distribution of MSCT frequencies was skewed toward high frequency sites (Fig. 2C). A Poisson model was used to generate an expected distribution of MSCT frequencies by assuming all sites had an equal probability of activity (Fig. 2C). Comparison of the distributions indicated that a Poisson model was unable to describe the data, confirming a highly nonrandom distribution of MSCT frequency. The data shown in Fig. 2 are from a single cell and are representative of data from six neurons.

In previous examples (Murphy et al. 1994, 1995), we have used low extracellular Mg^{2+} medium to unblock NMDA receptors (Mayer et al. 1984; Nowak et al. 1984) and promote Ca^{2+} influx through NMDA receptors to observe MSCTs. This condition was chosen to ensure that the highest signal to noise response would be available for analysis. However, low Mg^{2+} conditions are of course not physiological. Therefore, using more physiological conditions (1 mM extracellular Mg^{2+}) we report a low frequency of MSCTs at negative holding potentials (–80 or –70 mV; Fig. 3). If the neuron was depolarized to –35 mV, robust Ca^{2+} transients, which resembled those observed in the absence of Mg^{2+}, were readily apparent (n = 4 neurons). In these experiments we have added antagonists (Triggle and Jannis 1987) to block noninactivating L-type voltage-sensitive Ca^{2+} channels that would be expected to open at –35 mV. This experiment is consistent with results presented by others, such as Yuste and Denk (1995) and Schiller et al. (1998), who demonstrate that a pairing of action potentials and synaptic stimulation results in enhanced NMDA receptor activity (and Ca^{2+} influx) presumably as a result of relief of the Mg^{2+} block.

Discussion

Our results indicate that optical imaging of single quantal events in CNS neurons is feasible. Detection of these events arises through the high permeability of NMDA receptors to Ca^{2+} ions and the small volume of postsynaptic structures such as spines. As $[Ca^{2+}]_i$ is normally tightly regulated within a neuron, a large gradient for Ca^{2+} influx exists. Coupled with exquisitely sensitive detectors of $[Ca^{2+}]_i$ (Minta et al. 1989), we argue that it is possible to resolve quantal events associated with the opening of a single NMDA receptor channel (Fig. 1A and Methods). Direct measurement of $[Ca^{2+}]_i$ using fura-2 indicated that Ca^{2+} changes within spines were within 100–2000 μM levels and suggests the involvement of only a small number of receptors (Murphy et al. 1994, 1995). For example, if we assume that fura-2 is the dominant buffer in the cell, then we can estimate the amount of Ca^{2+} in the cytoplasm on the basis of the moles of fura-2 that are present. Calculations based on Ca^{2+}-induced changes in fura-2 fluorescence suggest that several hundred micromolar of fura-2 interact with Ca^{2+} at a synaptic site (200 μM = 2.0×10^{-19} mol, given a 1×10^{-15} L spine volume). This number would be equivalent to 120 000 Ca^{2+} ions binding to the dye. This quantity of Ca^{2+} is comparable with that entering a single open NMDA receptor (310 000 over 200 ms, Fig. 1A). Therefore, we confirm that Ca^{2+} entry through a small number of receptors is sufficient to trigger MSCTs. Calculations based on Ca^{2+}-bound fura-2 would likely underestimate the number of ions that interact with the dye because of additional cellular Ca^{2+} buffers and pumps. Thus, the estimates based on Ca^{2+}-bound fura-2 combined with direct measures of current amplitude are proof of the exquisite sensitivity of our imaging method. Consistent with our measurements and calculations Petrozzino et al. (1995) observed μM $[Ca^{2+}]_i$ levels in dendritic spines with repeated synaptic stimulation. A potential limitation of our direct measurement of currents that temporally correlate with MSCTs is the possibility that some of these currents may reflect activity at AMPA-type glutamate receptors. However, we believe that this potential error would be small as a result of the rapid kinetics of AMPA receptors (small total charge influx) and the presence of a large proportion of synapses that contain only NMDA-type receptors (Wang and Murphy 1998). This potential error would also tend to overestimate the number of NMDA receptors that are associated with MSCTs.

Analysis of MSCT frequencies using the Poisson model indicates a highly nonrandom distribution across responsive sites, suggesting that different synapses within cultured CNS neurons do not have equal probabilities of spontaneous miniature activity. In fact, synapses can differ by >10-fold with respect to their frequency of miniature synaptic events. Our results which directly demonstrate differences in miniature release probability are consistent with those obtained using other measures, such as time-dependent block of evoked synaptic currents by MK-801 (Rosenmund et al. 1993; Hessler et al. 1993). We have previously reported this nonuniform probability, using statistical analysis of pooled data from multiple cells (Murphy et al. 1994). In the current experiments using a slower sampling rate and confocal microscopy we have clearly established large differences in MSCT frequency between synapses within a single cell. The mechanism of this apparent difference in MSCT frequency is likely presynaptic since sites that show a lower frequency of events do not necessarily show them at lower amplitude (data not shown). This is an important observation since it would be possible for all sites to have an equal frequency of activity, but only the largest amplitude events being detected. Presynaptic mechanisms for the apparent high rate of miniature activity at some synapses may include elevated presynaptic terminal resting $[Ca^{2+}]_i$ (Atluri and Regehr 1998). Although greater than 10-fold differences in response frequency are observed, we believe that this might be an underestimate of the true heterogeneity in miniature release rates, since some spines never show MSCTs over the sampling period and are apparently inactive. Since MSCTs are largely NMDA receptor mediated (Murphy et al. 1994, 1995), their apparent absence at some synapses suggests postsynaptic regulation of NMDA receptor function in a manner analogous to that proposed for AMPA receptors (Isaac et al. 1995; Liao et al. 1995; Wang et al. 1996). It is also possible that some of the heterogeneity in MSCT frequency may reflect differences between synapses in postsynaptic Ca^{2+} buffering and potential release of Ca^{2+} from intracellular stores.

Our previous studies (Murphy et al. 1994, 1995) have used the absence of extracellular Mg^{2+} to relieve Mg^{2+} block of the NMDA receptor, permitting local Ca^{2+} transients to be

resolved in dendritic spines. In this study we demonstrate that with modest depolarization to –35 mV, unblocking of the NMDA receptor occurs, allowing larger and more frequent MSCTs to be observed in the presence of physiological Mg^{2+} concentration. The observed change in MSCT frequency (with depolarization) is somewhat puzzling since an unblocking of postsynaptic NMDA receptors would not be expected to have an effect on frequency of transmitter release. However, we believe that the reduction in MSCT amplitude associated with Mg^{2+} block may reduce event detection. Thus, a reduction in amplitude at hyperpolarized membrane potentials may also appear as a reduction in event frequency. In the presence of Mg^{2+} we occasionally observed MSCTs at negative holding potentials; it is possible that these events may result from local depolarization and reduction in Mg^{2+} block. It is also possible that a small number of synapses express Ca^{2+}-permeable AMPA-type glutamate receptors (Schneggenburger et al. 1993). We anticipate that when postsynaptic action potentials occur concurrently with synaptic stimulation, as shown by Yuste and Denk (1995) and recently by Schiller et al. (1998), similar NMDA receptor dependent Ca^{2+} transients would result from minimal synaptic stimulation. In fact we have described (Mackenzie et al. 1996) NMDA receptor antagonist sensitive Ca^{2+} transients associated with minimal stimulation at depolarized potentials, using a protocol similar to that employed by Malinow et al. (1994). In summary, our results suggest that the small volume of the dendritic spine, coupled with the high Ca^{2+} permeability of the NMDA receptor, permits the optical detection of quantal synaptic transmission within CNS neurons.

Acknowledgments

T.H.M. is supported by an operating grant from the Medical Research Council of Canada and is an EJLB Foundation and Medical Research Council of Canada scientist. O.P. is supported by a Deutscher Akademischer Austauschdienst (HSP-III) scholarship. S.W. is supported by a research fellowship from the Heart and Stroke Foundation of British Columbia and Yukon.

References

Alford, S., Frenguelli, B.G., Schofield, J.G., and Collingridge, G.L. 1993. Characterization of Ca^{2+} signals induced in hippocampal CA1 neurons by the synaptic activation of NMDA receptors. J. Physiol. (London), **469**: 693–716.

Atluri, P.P., and Regehr, W.G. 1998. Delayed release of neurotransmitter from cerebellar granule cells. J. Neurosci. **18**: 8214–8227.

Bekkers, J.M., and Stevens, C.F. 1989. NMDA and non-NMDA receptors are co-localized at individual excitatory synapses in cultured rat hippocampus. Nature (London), **341**: 230–233.

Edwards, F.A. 1995. Anatomy and electrophysiology of fast central synapses lead to a structural model for long-term potentiation. Physiol. Rev. **75**: 759–787.

Forti, L., Bossi, M., Bergamaschi, A., Villa, A., and Malgaroli, A. 1997. Loose-patch recordings of single quanta at individual hippocampal synapses. Nature (London), **388**: 874–878.

Garaschuk, O., Schneggenburger, R., Schirra, C., Tempia, F., and Konnerth, A. 1996. Fractional Ca^{2+} currents through somatic and dendritic glutamate receptor channels of rat hippocampal CA1 pyramidal neurones. J. Physiol. (London), **491**: 757–772.

Grynkiewicz, G., Poenie, M., and Tsien, R.Y. 1985. A new generation of Ca^{2+} indicators with greatly improved fluorescence properties. J. Biol. Chem. **260**: 3440–3450.

Hamill, O.P., Marty, A., Neher, E., Sakmann, B., and Sigworth, F. 1981. Improved patch-clamp techniques for high resolution current recordings from cells and cell-free membrane patches. Pfluegers Arch. Eur. J. Physiol. **391**: 85–100.

Harris, K.M., and Kater, S.B. 1994. Dendritic spines: cellular specializations imparting both stability and flexibility to synaptic function. Annu. Rev. Neurosci. **17**: 341–371.

Helmchen, F., Imoto, K., and Sakmann, B. 1996. Ca^{2+} buffering and action potential-evoked Ca^{2+} signaling in dendrites of pyramidal neurons. Biophys. J. **70**: 1069–1081.

Hessler, N.A., Shirke, A.M., and Malinow, R. 1993. The probability of transmitter release at a mammalian central synapse. Nature (London), **366**: 569–572.

Isaac, J.T.R., Nicoll, R.A., and Malenka, R.C. 1995. Evidence for silent synapses: implications for the expression of LTP. Neuron, **15**: 427–434.

Jaffe, D.B., and Brown, T.H. 1997. Calcium dynamics in thorny excrescences of CA3 pyramidal neurons. J. Neurophysiol. **78**: 10–18.

Jaffe, D.B., Fisher, S.A., and Brown, T.H. 1994. Confocal laser scanning microscopy reveals voltage-gated calcium signals within hippocampal dendritic spines. J. Neurobiol. **25**: 220–233.

Koch, C., and Zador, A. 1993. The function of dendritic spines: devices subserving biochemical rather than electrical compartmentalization. J. Neurosci. **13**: 413–422.

Koch, C., Zador, A., and Brown, T.H. 1992. Dendritic spines: convergence of theory and experiment. Science (Washington, D.C.), **256**: 973–974.

Lester, R.A., Clements, J.D., Westbrook, G.L., and Jahr, C.E. 1990. Channel kinetics determine the time course of NMDA receptor-mediated synaptic currents. Nature (London), **346**: 565–567.

Liao, D., Hessler, N.A., and Malinow, R. 1995. Activation of postsynaptically silent synapses during pairing-induced LTP in CA1 region of hippocampal slice. Nature (London), **375**: 400–404.

Lisman, J.E., and Harris, K.M. 1993. Quantal analysis and synaptic anatomy—integrating two views of hippocampal plasticity. Trends Neurosci. **16**: 141–147.

Mackenzie, P.J., and Murphy, T.H. 1998. High safety factor for action potential conduction along axons but not dendrites of cultured hippocampal and cortical neurons. J. Neurophysiol. **80**: 2089–2101.

Mackenzie, P.J., Umemiya, M., and Murphy, T.H. 1996. Calcium imaging of CNS axons in culture indicates reliable coupling between single action potentials and distal functional release sites. Neuron, **16**: 783–795.

Malinow, R., Otmakhov, N., Blum, K.I., and Lisman, J. 1994. Visualizing hippocampal synaptic function by optical detection of Ca^{2+} entry through the NMDA channel. Proc. Natl. Acad. Sci. U.S.A. **91**: 8170–8174.

Mayer, M.L., Westbrook, G.L., and Guthrie, P.B. 1984. Voltage-dependent block by Mg^{2+} of NMDA responses in spinal cord neurons. Nature (London), **309**: 261–263.

McBain, C.J., and Mayer, M.L. 1994. *N*-Methyl-D-aspartic acid receptor structure and function. Physiol. Rev. **74**: 723–760.

Minta, A., Kao, J., and Tsien, R.Y. 1989. Fluorescent indicators for cytosolic calcium based on rhodamine and fluorescein chromophores. J. Biol. Chem. **264**: 8171–8178.

Muller, W., and Connor, J.A. 1991. Dendritic spines as individual

neuronal compartments for synaptic Ca^{2+} responses. Nature (London), **354**: 73–76.

Murphy, T.H., and Baraban, J.M. 1990. Glutamate toxicity in immature cortical neurons precedes development of glutamate receptor currents. Dev. Brain Res. **57**: 146–150.

Murphy, T.H., Baraban, J.M., Wier, W.G., and Blatter, L.A. 1994. Visualization of quantal synaptic transmission by dendritic calcium imaging. Science (Washinton, D.C.), **263**: 529–532.

Murphy, T.H., Baraban, J.M., and Wier, W.G. 1995. Mapping miniature synaptic currents to single synapses using calcium imaging reveals heterogeneity in postsynaptic output. Neuron, **15**: 159–168.

Neher, E. 1995*a*. Voltage offsets in patch-clamp experiments. *In* Single-channel recording. *Edited by* B. Sakmann and E. Neher. Plenum Press, New York. pp. 147–153.

Neher, E. 1995*b*. The use of fura-2 for estimating Ca buffers and Ca fluxes. Neuropharmacology, **34**: 1423–1442.

Nowak, L.M., Bregestovski, P., Ascher, P., Herbert, A., and Prochiantz, A. 1984. Magnesium gates glutamate-activated channels in mouse central neurons. Nature (London), **307**: 462–465.

Petrozzino, J.J., Pozzo Miller, L.D., and Connor, J.A. 1995. Micromolar Ca^{2+} transients in dendritic spines of hippocampal pyramidal neurons in brain slice. Neuron, **14**: 1223–1231.

Raju, B., Murphy, E., Levy, L.A., Hall, R.D., and London, R.E. 1989. A fluorescent indicator for measuring cytosolic free magnesium. Am. J. Physiol. **256**: C540–C548.

Regehr, W.G., and Tank, D.W. 1990. Postsynaptic NMDA receptor-mediated calcium accumulation in hippocampal CA1 pyramidal cell dendrites. Nature (London), **345**: 807–810.

Robinson, H.P., Sahara, Y., and Kawai, N. 1991. Nonstationary fluctuation analysis and direct resolution of single channel currents at postsynaptic sites. Biophys. J. **59**: 295–304.

Rosenmund, C., Clements, J.D., and Westbrook, G.L. 1993. Nonuniform probability of glutamate release at a hippocampal synapse. Science (Washinton, D.C.), **262**: 754–757.

Schiller, J., Schiller, Y., and Clapham, D.E. 1998. NMDA receptors amplify calcium influx into dendritic spines during associative pre- and postsynaptic activation. Nature Neurosci. **1**: 114–118.

Schneggenburger, R., Zhou, Z., Konnerth, A., and Neher, E. 1993. Fractional contribution of calcium to the cation current through glutamate receptor channels. Neuron, **11**: 133–143.

Segal, M. 1995. Imaging of calcium variations in living dendritic spines of cultured rat hippocampal neurons. J. Physiol. (London), **486**: 283–295.

Silver, R.A., Traynelis, S.F., and Cull-Candy, S.G. 1992. Rapid-time-course miniature and evoked excitatory currents at cerebellar synapses in situ. Nature (London), **355**: 163–166.

Spruston, N., Jaffe, D.B., and Johnston, D. 1994. Dendritic attenuation of synaptic potentials and currents: the role of passive membrane properties. Trends Neurosci. **17**: 161–166.

Stevens, C.F. 1993. Quantal release of neurotransmitter and long-term potentiation. Cell **(**Suppl.), **72**: 55–63.

Svoboda, K., Tank, D.W., and Denk, W. 1996. Direct measurement of coupling between dendritic spines and shafts. Science (Washington, D.C.), **272**: 716–719.

Triggle, D.J., and Jannis, R.A. 1987. Calcium channel ligands. Annu. Rev. Pharmacol. Toxicol. **27**: 347–369.

Wang, S., and Murphy, T.H. 1998. Using GluR2 null mice to visualize AMPA synaptic activity at single CNS synapses. Soc. Neurosci. Abstr. **24**: 326.

Wang, S., Wojtowicz, J.M., and Atwood, H.L. 1996. Synaptic recruitment during long term potentiation at synapses of the medial peforant path in the dentate gyrus of the rat brain. Synapse, **21**: 78–86.

Yuste, R., and Denk, W. 1995. Dendritic spines as basic functional units of neuronal integration. Nature (London), **375**: 682–684.

Zador, A., Koch, C., and Brown, T.H. 1990. Biophysical model of a Hebbian synapse. Proc. Natl. Acad. Sci. U.S.A. **87**: 6718–6722.